INTERNAL EIGHT-BAND WWAN/LTE HANDSET ANTENNA USING LOOP SHORTING STRIP AND CHIP-CAPACITOR-LOADED FEEDING STRIP FOR BANDWIDTH ENHANCEMENT

Kin-Lu Wong and Yu-Wei Chang
Department of Electrical Engineering, National Sun Yat-Sen University, Kaohsiung 804, Taiwan; Corresponding author: wongkl@ema.ee.nsysu.edu.tw

Received 28 August 2010

ABSTRACT: *A planar inverted-F antenna (PIFA) with a loop shorting strip and a chip-capacitor-loaded feeding strip to achieve a small size yet wideband operation for eight-band WWAN/LTE operation (698960/17102690 MHz) in the mobile handset is presented. The antenna occupies a small no-ground footprint of 15 × 35 mm^2 on the main circuit board of the handset and is closely integrated with the surrounding system ground plane to achieve compact integration inside the handset. By applying the proposed shorting strip and feeding strip, a dual-resonance excitation at about 800 MHz which forms the antenna's wide lower band to cover the LTE700/GSM850/900 operation is obtained. Further, the proposed shorting strip and feeding strip lead to the generation of additional higher-order resonant modes to assist in forming a wide upper band for the antenna to cover the GSM1800/1900/UMTS/LTE2300/2500 operation. The proposed antenna also shows good radiation characteristics over the eight operating bands. The obtained SAR values of the antenna are well less than the limit of 1.6 W/kg for 1-g head tissue for practical handset applications.* © 2011 Wiley Periodicals, Inc. Microwave Opt Technol Lett 53:1217–1222, 2011; View this article online at wileyonlinelibrary.com. DOI 10.1002/mop.25983

Key words: *internal handset antennas; WWAN antennas; LTE antennas; loop shorting strip; chip-capacitor-loaded feeding strip*

1. INTRODUCTION

Planar inverted-F antennas with no back ground plane have been shown to be very suitable to be directly disposed on the no-ground portion of the main circuit board of the mobile handset for penta-band wireless wide area network (WWAN) or eight-band WWAN/LTE (long-term evolution) operation [1–7]. However, these internal antennas are generally required to occupy the entire top or bottom edge of the main circuit board of the handset, similar to many internal WWAN handset antennas [8–14]. This is mainly because such antennas require enough isolation space to nearby system ground plane to obtain negligible coupling effects between the antenna's radiating portion and the nearby system ground plane [15–20]. This design requirement limits the compact integration of the internal antenna with nearby electronic components inside the handset. This also causes an increase of the total occupied volume of the internal antenna inside the handset.

In this article, we present an onboard internal WWAN/LTE antenna with a small size (15 × 35 mm^2) to closely integrate with the surrounding ground plane of the handset. No isolation space between the internal antenna and the surrounding ground plane is generally required. That is, the total occupied board space of the internal antenna is the same as the antenna's metal pattern disposed on the main circuit board. The small size and wideband operation of the internal WWAN/LTE antenna is achieved by applying a loop shorting strip and a chip-capacitor-loaded feeding strip to replace the simple shorting strip and feeding strip of the traditional planar inverted-F antenna. The proposed shorting strip and feeding strip result in a dual-resonance excitation at about 800 MHz for the antenna to have a wide lower band to cover the LTE700/GSM850/900 operation (698960 MHz). In addition, additional higher-order resonant modes are excited to assist in forming a wide upper band to cover the GSM1800/1900/UMTS/LTE2300/2500 operation (17102690 MHz). The antenna can hence cover eight-band WWAN/LTE operation. Details of the planar inverted-F antenna with the proposed loop shorting strip and chip-capacitor-loaded feeding strip are described in the article. The antenna is also fabricated and tested, and the obtained results are presented. The antenna's radiation characteristics including the specific absorption rate (SAR) values for 1-g head tissue [21] are also studied.

2. PROPOSED ANTENNA

Figure 1 shows the geometry of the proposed internal eight-band LTE/WWAN handset antenna. The antenna comprises a radiating strip, a loop shorting strip between points B and E, and a chip-capacitor-loaded feeding strip between points A and D. Note that Point B is the shorting point which is short circuited to the main ground plane printed on the back surface of the main circuit board. In this study, a 0.8-mm thick FR4 substrate of relative permittivity 4.4, loss tangent 0.02, and size 115 × 60 mm^2 is used to simulate the main circuit board of the handset. The main ground plane has a size of 100 × 60 mm^2 and combines with the extended ground plane of size 15 × 25 mm^2 to form the system ground plane of the handset. The antenna's metal pattern (radiating strip, shorting strip, and feeding strip) is closely surrounded by the system ground plane. No isolation space is generally required between the antenna and the surrounding ground plane, which makes the antenna occupy a small no-ground board space of 15 × 35 mm^2 on the main circuit board. With the proposed design, the extended ground plane can be used to accommodate nearby electronic elements such as the loudspeaker [22, 23], lens of the embedded digital camera [15, 24], universal serial bus (USB) connecter [25, 26] as the data port, and so on. This can lead to more degrees of freedom in arranging the internal antenna inside the handset and more compact integration of the internal antenna with the associated electronic elements inside the handset.

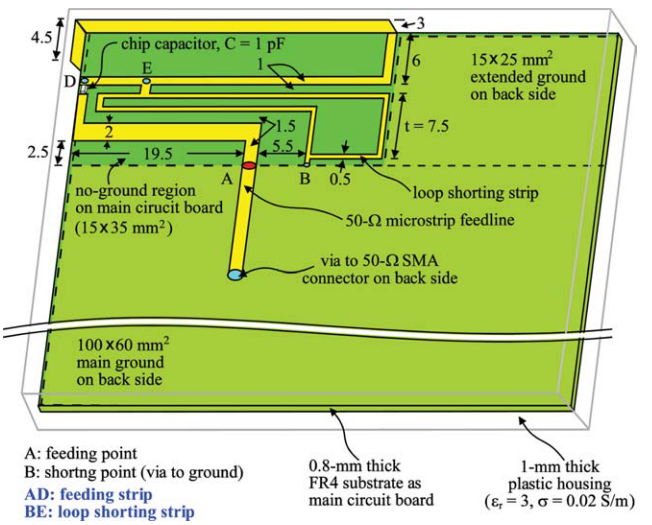

Figure 1 Geometry of the proposed internal eight-band LTE/WWAN handset antenna. [Color figure can be viewed in the online issue, which is available at wileyonlinelibrary.com]

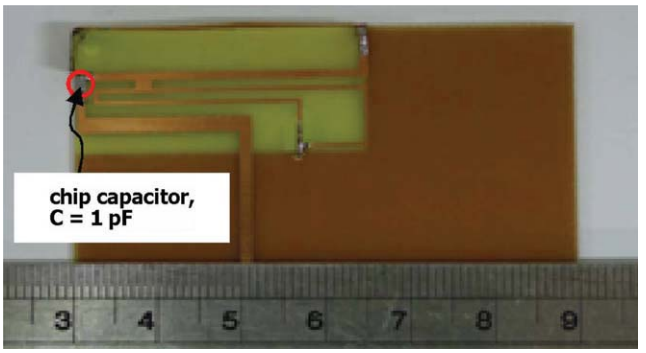

Figure 2 Photo of the fabricated antenna (handset casing not included in the photo). [Color figure can be viewed in the online issue, which is available at wileyonlinelibrary.com]

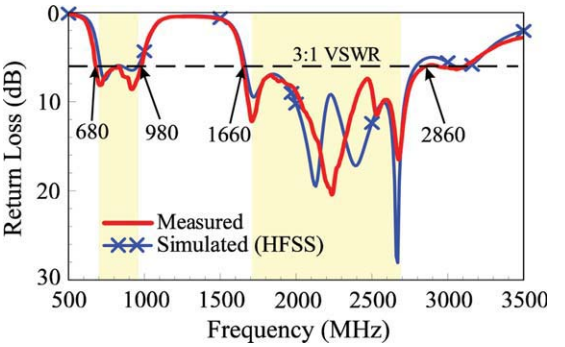

Figure 3 Measured and simulated return loss for the proposed antenna. [Color figure can be viewed in the online issue, which is available at wileyonlinelibrary.com]

The radiating strip of the antenna is selected to have a length close to 0.25 wavelength at about 800 MHz. Note that to achieve a small required footprint on the main circuit board, a portion of the radiating strip of 3 mm in width is perpendicularly mounted along the edge of the main circuit board. This decreases the required no-ground portion on the main circuit board to be 15 $\times$ 35 mm^2 only. By using the chip-capacitor-loaded feeding strip, which provides capacitive coupling to excite the antenna, a dual-resonance excitation at about 800 MHz can be obtained. The chip capacitor used in the study is 1 pF, and the contributed capacitive coupling to the antenna is similar to the reported coupled-fed internal handset antennas using a distributed coupling feed [1–7, 27–29].

The capacitive coupling can decrease the high input impedance level of the excited resonant mode at about 850 MHz. When the distributed coupling feed with a long coupling length is used, large decrease of both the real and imaginary parts of the input impedance of the excited resonant mode at about 800 MHz (the antenna's fundamental or lowest resonant mode) can be obtained. This can lead to a dual-resonance excitation with good impedance matching at about 800 MHz so that a wide lower band for the antenna can be obtained. By using the chip capacitor to replace the printed distributed coupling feed with a long coupling length, the dual-resonance excitation of the antenna's fundamental resonant mode can still be obtained. However, the impedance matching of the excited dual-resonance cannot be as good as that of using the distributed coupling feed with a long coupling length [1–7, 27–29]. By further applying the loop shorting strip between points B and E, much improved impedance matching of the excited dual-resonance of the antenna's fundamental resonant mode can be obtained. This impedance matching improvement is obtained largely because the loop shorting strip leads to smoother distribution of the excited surface currents on the shorting strip, which is helpful in decreasing the input impedance level of the exited resonant mode. Hence, by using both the chip-capacitor-loaded feeding strip and loop shorting strip, a wide lower band to cover the desired 698960 MHz band is obtained for the antenna.

Also note that the loop shorting strip provides two long but different paths to short-circuit the radiating strip to the main ground plane. This leads to additional higher-order resonant modes of the antenna excited to assist in forming a wide upper band to cover the desired 17102690 MHz. This is an advantage over the reported coupled-fed internal handset antennas using a distributed coupling feed and a simple shorting strip [6, 7], in which the obtained upper band cannot provide a very wide bandwidth of larger than 1 GHz to cover the desired GSM850/900/1800/1900/UMTS operation. In addition, the proposed shorting strip can be very close to the surrounding ground plane, so is the radiating strip whose front section is close to the surrounding ground plane. This arrangement leads to compact integration of the proposed antenna with the surrounding ground plane on the main circuit board. The reason for this attractive feature is obtained largely because there are generally strong excited surface currents on the shorting strip and the front section of the radiating strip. Because strong surface currents generally leads to weak electric fields generated in the near-field region [30], the coupling between the antenna and the surrounding ground plane will become small. In this case, close

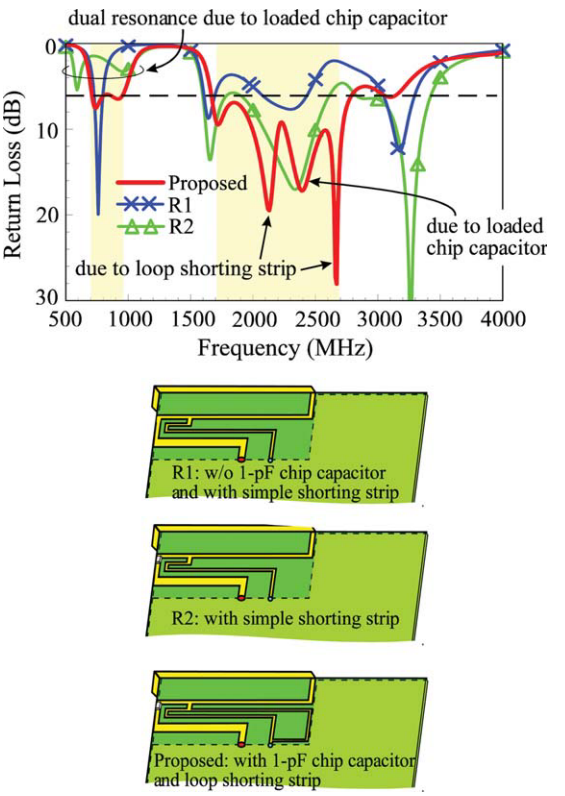

Figure 4 Comparison of the simulated return loss for the proposed antenna, the case without the loaded chip capacitor and with a simple shorting strip (R1), and the case with a simple shorting strip (R2). [Color figure can be viewed in the online issue, which is available at wileyonlinelibrary.com]

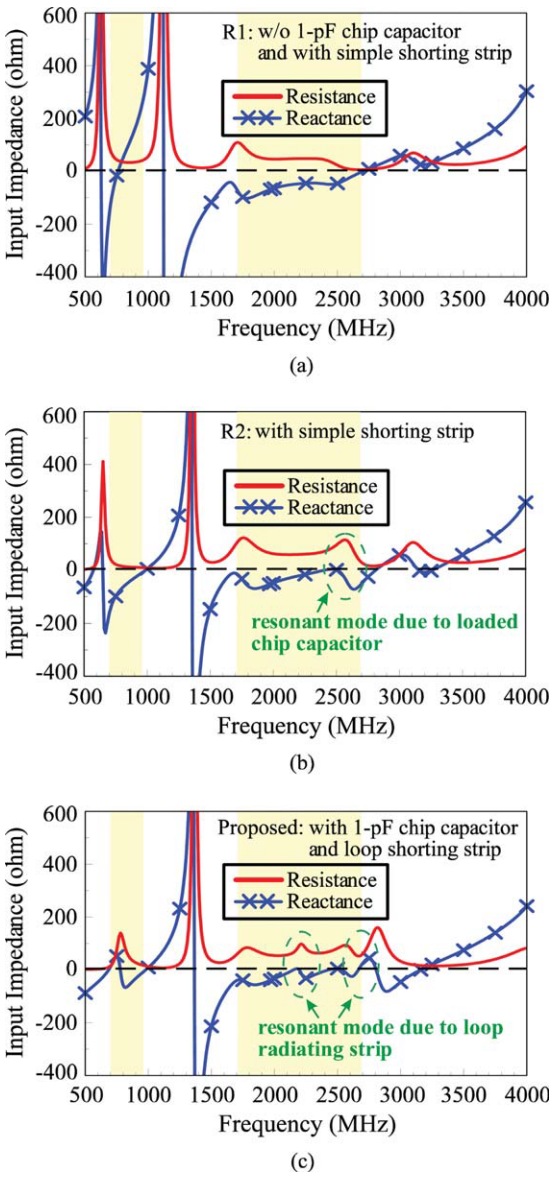

Figure 5 Simulated input impedance of the three antennas studied in Figure 4. [Color figure can be viewed in the online issue, which is available at wileyonlinelibrary.com]

proximity of the antenna to the surrounding ground plane becomes possible.

To simulate the practical handset casing in the experiment, a plastic casing of thickness 1 mm, relative permittivity 3.0, and conductivity 0.02 S/m is made to enclose the main circuit board as shown in Figure 1. The photo of the fabricated antenna is shown in Figure 2 (the handset casing is not included). To test the antenna, a short 50-Ω microstrip feedline is printed on the front surface of the main circuit board, with one end connected to the antenna at the feeding point (Point A) and the other end connected to a 50-Ω SMA connector on the back side of the main circuit board. The obtained results of the fabricated antenna are presented in Section 3.

3. RESULTS AND DISCUSSION

Figure 3 shows the measured and simulated return loss for the proposed antenna. The simulated results are obtained using simulation software HSFF (high frequency structure simulator) version 12 [31] and are in agreement with the measured data. Over the desired WWAN/LTE bands (shown by the two shaded frequency ranges in the figure), the obtained input impedance is better than 3:1 VSWR or 6-dB return loss, which is widely used as the design specification for the internal WWAN/LTE handset antenna.

To analyze the operating principle of the proposed antenna, Figure 4 shows the comparison of the simulated return loss for the proposed antenna, the case without the loaded chip capacitor and with a simple shorting strip ($R1$), and the case with a simple shorting strip ($R2$). For the case of $R1$, which uses a simple feeding strip and a simple shorting strip, the excited resonant mode in the desired lower band has a narrow bandwidth and is far from covering the desired 698960 MHz band. The narrow bandwidth is mainly owing to the very high input impedance level of the excited resonant mode in the desired lower band [see the simulated input impedance of $R1$ shown in Fig. 5(a)].

By loading a 1-pF chip capacitor in the feeding strip (the case of $R2$), dual-resonance excitation of the resonant mode can be obtained, although the impedance matching needs to be improved. This behavior is owing to the decreased input impedance level of the excited resonant mode in the desired lower band [see the simulated input impedance of R2 shown in Fig. 5(b) compared to that of R1 in Fig. 5(a)]. In addition, some improvement in the impedance matching for frequencies over the desired 17102690 MHz band is obtained. By further applying the loop shorting strip, improved impedance matching of the dual-resonance excitation in the lower band is obtained, which results in a wide operating band obtained. This behavior is owing to the much lowered input impedance level of the excited resonant mode in the lower band [see the simulated input impedance of R1 shown in Fig. 5(c)]. Further, additional higher-

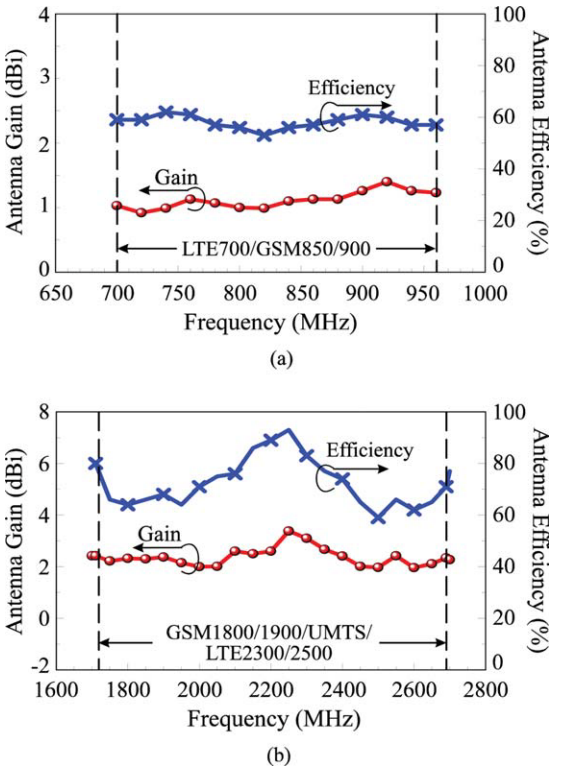

Figure 6 Measured antenna gain and antenna efficiency (mismatching loss included) for the proposed antenna. (a) The lower band (698960 MHz). (b) The upper band (17102690 MHz). [Color figure can be viewed in the online issue, which is available at wileyonlinelibrary.com]

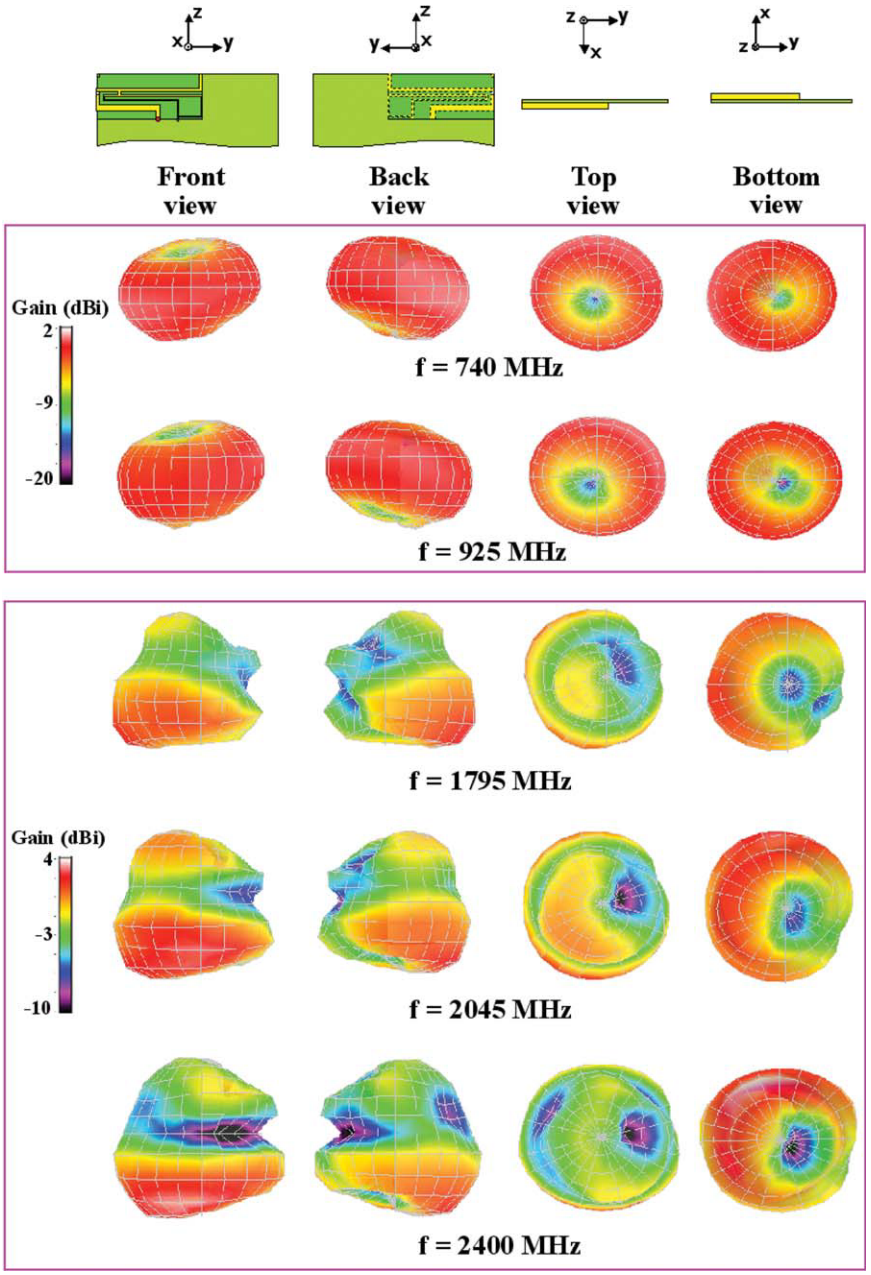

Figure 7 Measured 3-D total-power radiation patterns for the proposed antenna. [Color figure can be viewed in the online issue, which is available at wileyonlinelibrary.com]

order resonant modes at about 2100 and 2700 MHz are excited in the desired upper band [see Fig. 5(c)]. The additional resonant modes make the antenna's upper band have a wide bandwidth of larger than 1 GHz to cover the desired 17102690 MHz band.

The measured antenna gain and antenna efficiency for the proposed antenna are shown in Figure 6. The antenna is tested in a far-field anechoic chamber, and the measured antenna gain and antenna efficiency include the mismatching loss. Over the desired lower band shown in Figure 6(a), the antenna gain varies from about 0.9 to 1.3 dBi, and the antenna efficiency varies from about 53 to 61%. Although over the desired upper band shown in Figure 6(b), the antenna gain is about 2.0 to 3.2 dBi, and the antenna efficiency is about 60 to 92%. The measured three-dimensional total-power radiation patterns at typical frequencies are presented in Figure 7. At 740 and 925 MHz in the lower band, the radiation patterns are similar to those of the traditional half-wavelength dipole mode. At 1795, 2045, and 2400 MHz in the upper band, because there are surface current nulls in the system ground plane, the radiation patterns are close to those of the traditional higher-order dipole modes. Some nulls or dips in the azimuthal plane (x–y plane) are seen, which are different from the omnidirectional radiation seen at lower frequencies. The obtained radiation patterns show no special distinctions to those of the traditional internal WWAN handset antennas that have been reported [32].

Figure 8 shows the SAR simulation model and the simulated SAR values for 1-g head tissue. The input power and return loss at each testing frequency are also shown in the table. The SAR simulation model is provided by SEMCAD X version 14 [33].

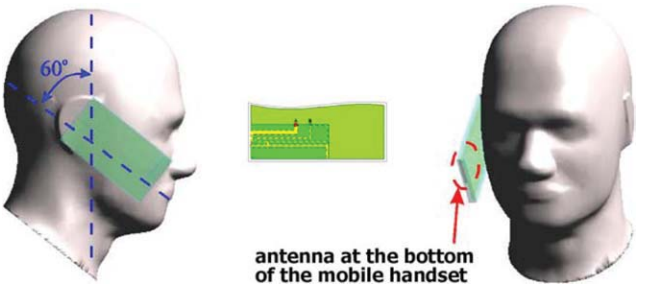

Figure 8 SAR simulation model and the simulated SAR values for 1-g head tissue. [Color figure can be viewed in the online issue, which is available at wileyonlinelibrary.com]

Note that since the related internal antennas with no back ground plane is especially attractive to be placed at the bottom edge of the handset to obtain decreased SAR values [1, 3, 6], the proposed antenna is disposed at the corner of the bottom edge of the handset as shown in the simulation model. The simulated 1-g head tissue SAR values are listed in the table. The results are well below the limit of 1.6 W/kg [21]. This indicates that the proposed antenna is promising for practical handset applications.

Finally, a parametric study for the loaded chip capacitor and the loop shorting strip is conducted. Figure 9 shows the simulated return loss for the proposed antenna as a function of the capacitance of the loaded chip capacitor in the feeding strip. Results for the capacitance varied from 0.47 to 1.5 pF are presented in the figure. There are large effects on the dual-resonance excitation of the resonant mode in the lower band. When the chip capacitor with a smaller capacitance is loaded (for example, $C = 0.47$ pF in the figure), dual-resonance excitation cannot be obtained for the resonant mode in the lower band. On the other hand, when the chip capacitor with a larger capacitance is loaded ($C = 1.5$ pF in the figure), good impedance matching for the dual-resonance excitation of the excited resonant mode cannot be achieved. By selecting a proper value of the loaded capacitance ($C = 1.0$ pF in this study), acceptable impedance matching for frequencies over the desired lower band can be obtained. For the upper band, the effects of the loaded chip capacitance are relatively small, as the impedance matching over the desired 17102690 MHz band for the three cases studied meets the design specification of 6-dB return loss.

Results of the simulated return loss as a function of the length t in the loop shorting strip are presented in Figure 10.

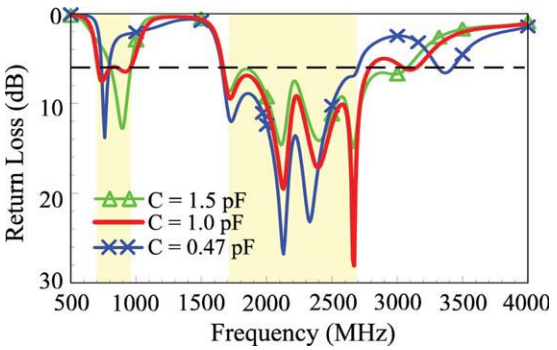

Figure 9 Simulated return loss for the proposed antenna as a function of the capacitance of the loaded chip capacitor in the feeding strip. [Color figure can be viewed in the online issue, which is available at wileyonlinelibrary.com]

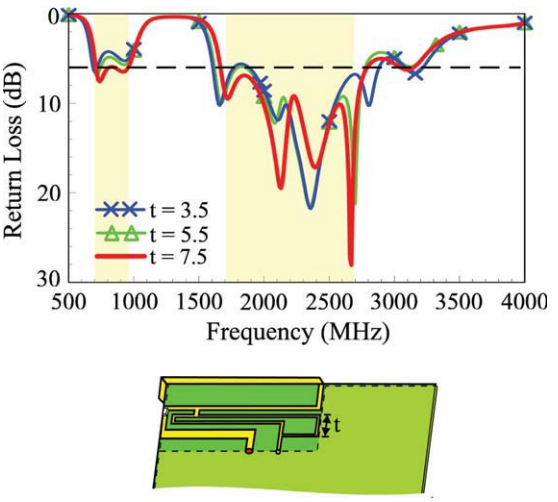

Figure 10 Simulated return loss for the proposed antenna as a function of the length t in the loop shorting strip. [Color figure can be viewed in the online issue, which is available at wileyonlinelibrary.com]

Results for the length t varied from 3.5 to 7.5 mm are shown. Similar to the results in Figure 9, large effects on the impedance matching of the lower band are seen, whereas the effects on the impedance matching of the upper band are small. The results shown in Figures 9 and 10 indicate that both the loaded chip capacitor and the loop shorting strip contribute significantly to the good dual-resonance excitation of the resonant mode in the lower band. For the upper band, although the presence of both the loaded chip capacitor and the loop shorting strip are crucial for obtaining a large bandwidth (>1 GHz), small variations in the capacitance of the loaded chip capacitor and the length of the loop shorting strip will not cause significant variations in the obtained upper-band bandwidth. This feature is attractive as it makes the fine adjustment of the required bandwidths of both the lower and upper bands easy to achieve.

4. CONCLUSIONS

An on-board internal inverted-F antenna having a small footprint of 15 × 35 mm^2 on the main circuit board of the handset and two wide operating bands for eight-band WWAN/LTE operation (698960/17102690 MHz) has been proposed. The wide bandwidths of the antenna are obtained by using a loaded chip capacitor in the shorting strip and a loop shorting strip replacing the traditional simple shorting strip. Further, the antenna can be closely integrated with surrounding ground plane with no isolation space required. This feature leads to compact integration of the antenna inside the handset and also efficient antenna and circuit layout planning on the main circuit board of the handset. Acceptable radiation characteristics over the eight operating bands of WWAN/LTE have also been obtained. The SAR values for 1-g head tissue for the antenna disposed at the bottom edge of the handset have also been studied. The simulated SAR results are well below the limit of 1.6 W/kg, making the antenna very promising for practical handset applications.

REFERENCES

1. K.L. Wong, W.Y. Chen, C.Y. Wu, and W.Y. Li, Small-size internal eight-band LTE/WWAN mobile phone antenna with internal distributed LC matching circuit, Microwave Opt Technol Lett 52 (2010), 2244–2250.

2. K.L. Wong, M.F. Tu, C.Y. Wu, and W.Y. Li, Small-size coupled-fed printed PIFA for internal eight-band LTE/GSM/UMTS mobile phone antenna, Microwave Opt Technol Lett 52 (2010), 2123–2128.
3. S.C. Chen and K.L. Wong, Bandwidth enhancement of coupled-fed on-board printed PIFA using bypass radiating strip for eight-band LTE/GSM/UMTS slim mobile phone, Microwave Opt Technol Lett 52 (2010), 2059–2065.
4. T.W. Kang and K.L. Wong, Simple small-size coupled-fed uniplanar PIFA for multiband clamshell mobile phone application, Microwave Opt Technol Lett 51 (2009), 2805–2810.
5. C.T. Lee and K.L. Wong, Uniplanar coupled-fed printed PIFA for WWAN/WLAN operation in the mobile phone, Microwave Opt Technol Lett 51 (2009), 1250–1257.
6. C.H. Chang and K.L. Wong, Printed λ/8-PIFA for penta-band WWAN operation in the mobile phone, IEEE Trans Antennas Propag 57 (2009), 1373–1381.
7. K.L. Wong and C.H. Huang, Printed PIFA with a coplanar coupling feed for penta-band operation in the mobile phone, Microwave Opt Technol Lett 50 (2008), 3181–3186.
8. N. Takemura, Inverted FL antenna with self-complementary structure, IEEE Trans Antennas Propag 57 (2009), 3029–3034.
9. R.A. Bhatti, Y.T. Im, and S.O. Park, Compact PIFA for mobile terminals supporting multiple cellular and non-cellular standards, IEEE Trans Antennas Propag 57 (2009), 2534–2540.
10. A. Cabedo, J. Anguera, C. Picher, M. Ribo, and C. Puente, Multiband handset antenna combining a PIFA, slots, and ground plane modes, IEEE Trans Antennas Propag 57 (2009), 2526–2533.
11. X. Zhang and A. Zhao, More stabilized triple-band antenna with a rolled radiating arm and a metallic rod for mobile applications, Microwave Opt Technol Lett 51 (2009), 891–894.
12. C.L. Liu, Y.F. Lin, C.M. Liang, S.C. Pan, and H.M. Chen, Miniature internal penta-band monopole antenna for mobile phones, IEEE Trans Antennas Propag 58 (2010), 1008–1011.
13. S. Hong, W. Kim, H. Park, S. Kahng, and J. Choi, Design of an internal multiresonant monopole antenna for GSM900/DCS1800/US-PCS/S-DMB operation, IEEE Trans Antennas Propag 56 (2008), 1437–1443.
14. M. Z. Azad and M. Ali, A miniaturized Hilbert PIFA for dual-band mobile wireless applications, IEEE Antennas Wireless Propag Lett 4 (2005), 59–62.
15. C.M. Su, K.L. Wong, C.L. Tang, and S.H. Yeh, EMC internal patch antenna for UMTS operation in a mobile device, IEEE Trans Antennas Propag 53 (2005), 3836–3839.
16. K.L. Wong and C.H. Chang, An EMC foam-base chip antenna for WLAN operation, Microwave Opt Technol Lett 47 (2005), 80–82.
17. K.L. Wong and C.H. Chang, Surface-mountable EMC monopole chip antenna for WLAN operation, IEEE Trans Antennas Propag 54 (2006), 1100–1104.
18. C.M. Su, K.L. Wong, B. Chen, and S. Yang, EMC internal patch antenna integrated with a U-shaped shielding metal case for mobile device application, Microwave Opt Technol Lett 48 (2006), 1157–1161.
19. C.I. Lin, K.L. Wong, S.H. Yeh, and C.L. Tang, Study of an L-shaped EMC chip antenna for UMTS operation in a PDA phone with the user's hand, Microwave Opt Technol Lett 48 (2006), 1746–1749.
20. K.L. Wong, C.H. Chang, and Y.C. Lin, Printed PIFA EM compatible with nearby conducting elements, IEEE Trans Antennas Propag 55 (2007), 2919–2922.
21. American National Standards Institute (ANSI), Safety levels with respect to human exposure to radio-frequency electromagnetic field, 3 kHz to 300 GHz, ANSI/IEEE standard C95.1, April 1999.
22. C.H. Wu and K.L. Wong, Internal shorted planar monopole antenna embedded with a resonant spiral slot for penta-band mobile phone application, Microwave Opt Technol Lett 50 (2008), 529–536.
23. Y.W. Chi and K.L. Wong, Half-wavelength loop strip fed by a printed monopole for penta-band mobile phone antenna, Microwave Opt Technol Lett 50 (2008), 2549–2554.
24. S.L. Chien, F.R Hsiao, Y.C. Lin, and K.L. Wong, Planar inverted-F antenna with a hollow shorting cylinder for mobile phone with an embedded camera, Microwave Opt Technol Lett 41 (2004), 418–419.
25. Available at: http://www.usb.org/, Universal Serial Bus (USB).
26. K.L. Wong and C.H. Chang, On-board small-size printed monopole antenna integrated with USB connector for penta-band WWAN mobile phone, Microwave Opt Technol Lett 52 (2010), 2523–2527.
27. C.H. Chang and K.L. Wong, Internal coupled-fed shorted monopole antenna for GSM850/900/1800/1900/UMTS operation in the laptop computer, IEEE Trans Antennas Propag 56 (2008), 3600–3604.
28. C.T. Lee and K.L. Wong, Internal WWAN clamshell mobile phone antenna using a current trap for reduced groundplane effects, IEEE Trans Antennas Propag 57 (2009), 3303–3308.
29. C.T. Lee and K.L. Wong, Planar monopole with a coupling feed and an inductive shorting strip for LTE/GSM/UMTS operation in the mobile phone, IEEE Trans Antennas Propag 58 (2010), 2479–2483.
30. T. Yang, W.A. Davis, W.L. Stutzman, and M.C. Huynh, Cellular-phone and hearing-aid interaction: an antenna solution, IEEE Antennas Propag Mag 50 (2008), 51–65.
31. Available at: http://www.ansoft.com/products/hf/hfss/, Ansoft Corporation HFSS, Pittsburgh, PA.
32. K.L. Wong, Planar antennas for wireless communications, Wiley, New York, 2003.
33. Available at: http://www.semcad.com, SPEAG SEMCAD, Schmid & Partner Engineering AG.

BROADBAND BLUETOOTH ANTENNA BASED ON CO_2Z HEXAFERRITE-GLASS COMPOSITE

Jaejin Lee,[1] Yang-Ki Hong,[1] Seok Bae,[1] Gavin S. Abo,[1] Jeevan Jalli,[1] Jihoon Park,[1] Won-Mo Seong,[2] Sang-Hoon Park,[2] Won-Gi An,[2] and Gi-Ho Kim[2]
[1] Department of Electrical and Computer Engineering and MINT Center, The University of Alabama, Tuscaloosa, Alabama 35487; Corresponding author: ykhong@eng.ua.edu
[2] Research and Development Center, EMW Co., Ltd., Kasan-Dong, Gumchon-Gu, Seoul, South Korea

Received 29 August 2010

ABSTRACT: *Bluetooth ferrite antenna was fabricated on Co_2Z ($Ba_3Co_2Fe_{24}O_{41}$) hexaferrite-glass composite substrate and characterized. The fabricated antenna has a total volume of 36 mm^3 (3 × 8 × 1.5 mm^3) and showed wide bandwidth (390 MHz at VSWR < 2). The maximum 3D peak-gain and radiation efficiency were measured to be 3.32 dBi at 2.35 GHz and 77.7% at 2.3 GHz, respectively. The 3D peak gain of 2.45 dBi and 3D average gain of −1.89 dBi were obtained at the Bluetooth central frequency of 2.45 GHz.* © 2011 Wiley Periodicals, Inc. Microwave Opt Technol Lett 53:1222–1225, 2011; View this article online at wileyonlinelibrary.com. DOI 10.1002/mop.25982

Key words: *bluetooth; ferrite antenna; Co_2Z hexaferrite; low magnetic loss; broad bandwidth*

1. INTRODUCTION

Small size and broadband GHz antennas have attracted great attention for wireless communications including wireless LAN and Bluetooth (2.4 ~ 2.483 GHz). Accordingly, dielectric antennas have been developed and commercialized for Bluetooth antenna [1]. However, the dielectric antenna shows narrower bandwidth (BW) of 18% and lower radiation efficiency (RE) of 78% than magneto-dielectric antenna due to the capacitive coupling between antenna and its ground plane [2], and embedded